New Zealand Journal of Marine and Freshwater Research

ISSN: 0028-8330 (Print) 1175-8805 (Online) Journal homepage: https://www.tandfonline.com/loi/tnzm20

Evaluation of four global ocean reanalysis products for New Zealand waters–A guide for regional ocean modelling

Joao Marcos Azevedo Correia de Souza, Phellipe Couto, Rafael Soutelino & Moninya Roughan

To cite this article: Joao Marcos Azevedo Correia de Souza, Phellipe Couto, Rafael Soutelino & Moninya Roughan (2020): Evaluation of four global ocean reanalysis products for New Zealand waters–A guide for regional ocean modelling, New Zealand Journal of Marine and Freshwater Research, DOI: 10.1080/00288330.2020.1713179

To link to this article: https://doi.org/10.1080/00288330.2020.1713179

Published online: 22 Jan 2020.

NEW ZEALAND JOURNAL OF MARINE AND FRESHWATER RESEARCH
https://doi.org/10.1080/00288330.2020.1713179

Taylor & Francis
Taylor & Francis Group

RESEARCH ARTICLE

Evaluation of four global ocean reanalysis products for New Zealand waters–A guide for regional ocean modelling

Joao Marcos Azevedo Correia de Souza [a], Phellipe Couto[a], Rafael Soutelino[b] and Moninya Roughan[c,d]

[a]A division of Meteorological Service of New Zealand, MetOcean Solutions, Raglan, New Zealand; [b]Oceanum Ltd, Raglan, New Zealand; [c]Meteorological Service of New Zealand, Auckland, New Zealand; [d]School of Mathematics and Statistics, University of New South Wales, Sydney, NSW, Australia

ABSTRACT

A comparison between 4 (near) global ocean reanalysis products is presented for the waters around New Zealand. The objective is to provide information for an educated choice of ocean estate estimate. The simulations are compared to satellite and *in situ* observations, and vertical sections are extracted to evaluate the representation of the main regional boundary currents and their transport. Overall, the Copernicus GLORYS reanalysis exhibits the better performance, with more realistic ocean variability and smaller biases in the water column structure. However, the BlueLink Reanalysis (BRAN) provides more realistic transport estimates of the East Auckland Current, an important boundary current connecting New Zealand to the World Ocean. All simulations have important biases in both temperature and salinity, particularly in coastal regions. Moreover, they are not able to represent coastal currents and processes. Therefore, the present study results emphasise the need for a regional ocean reanalysis and a data assimilative operational forecast system.

ARTICLE HISTORY
Received 10 June 2019
Accepted 3 January 2020

KEYWORDS
Ocean reanalysis; model evaluation; regional processes; dynamics; transport; ocean observations

Introduction

There is a growing demand for regional ocean models for scientific, societal and industry applications. Such models are designed with the appropriate resolution and physics to represent local processes commonly omitted from global simulations. In regions where such regional simulations are not available, global reanalyses are often used to provide a best estimate of the ocean currents. However, phenomena that are commonly not included in global simulations, such as tides, local wind forcing, coupling to surface waves, and the inverse barometer effect, can be important for coastal and regional applications. These include estimates of regional circulation and sea water temperature, and the prediction of storm surge. Furthermore, nested high resolution regional model grids are essential components of forecast systems, often providing gains in predictability with significant impacts on 'Search And Rescue' (SAR) or spill containment operations.

Several steps are necessary in the development of regional simulations. From tailored ocean bathymetry that includes local high resolution data sources, the selection of the

CONTACT Joao Marcos Azevedo Correia de Souza j.souza@metocean.co.nz

important physical processes to be represented, definition of model parameterizations and numerical schemes, to the choice of relevant forcing fields and appropriate boundary conditions. Further, Moore et al. (2019) emphasize that surface and lateral boundary conditions can represent a significant source of error in regional models. Regional domains without DA are particularly susceptible to such errors and biases introduced from global simulations.

Ocean boundary conditions for regional models are usually obtained from global ocean reanalysis products with DA. These systems compute an optimal ocean state estimate by combining the available broad scale observations within a dynamical framework provided by a numerical model. The core idea is to have a final product that overcomes the typical scarcity of ocean observations and the limitations of free-running numerical simulations. These simulations provide a particularly useful estimation of the dynamical state of the ocean in relatively data-poor regions, as is the case of New Zealand (Callaghan et al. 2019). Hence, such global simulations are used to include the contribution of the background large-scale mean circulation and external mesoscale features to the local dynamics. In particular for a long (multi-decadal) model integration, introduced variability at time scales from days to decades will be important. For example, Zhang et al. (2016) discusses how model drift derived from bias in surface forcing can lead to contamination of climate change signals. The same is true for open boundary conditions in nested regional domains.

A careful analysis of the available ocean reanalyses enables an objective choice among the various available products, which is key for minimising potential biases propagating into the regional nest. A few efforts have been made in recent years to contrast the results provided by the publicly available ocean reanalyses, with emphasis on the Ocean Reanalyses Intercomparison Project (ORA–IP). Balmaseda et al. (2015) provides a description of the project and its first results, identifying the ocean characteristics for which the ocean estate estimation is in general robust. Focusing on the period between 1993 and 2010, the authors show that higher horizontal resolution associated with assimilation of satellite data leads to a higher skill in estimating sea surface height when compared to tide gauges. Larger differences between reanalyses are noted in the tropics for the thermocline and mixed layer depth and the representation of the inter-annual salinity variability is also problematic. The deep ocean (below a few hundred metres), the Southern Ocean, coastal areas and western boundary currents–all essential to resolve the regional dynamics in New Zealand–were detected as areas of large uncertainty. The present study provides an in depth reanalysis intercomparison focussing in New Zealand waters.

The study area is the oceanic region around New Zealand, illustrated in Figure 1. A review on the physical oceanography of New Zealand waters is provided by Stevens et al. (2019). Given its dimensions and location in the South West Pacific basin, New Zealand regional circulation is subjected to significant influence of large scale flows. Given their typical horizontal resolution, global reanalyses with DA are expected to represent such dynamics with a significant degree of skill. However, the complex bathymetry, narrow continental shelf, and the high mesoscale variability adds complexities that are beyond the capability of relatively coarse global reanalysis, even considering comprehensive DA.

Since model performance is not geographically uniform and given that key areas impacting the waters around New Zealand could present important differences between reanalyses, a focussed comparison is necessary. Potential errors introduced through the

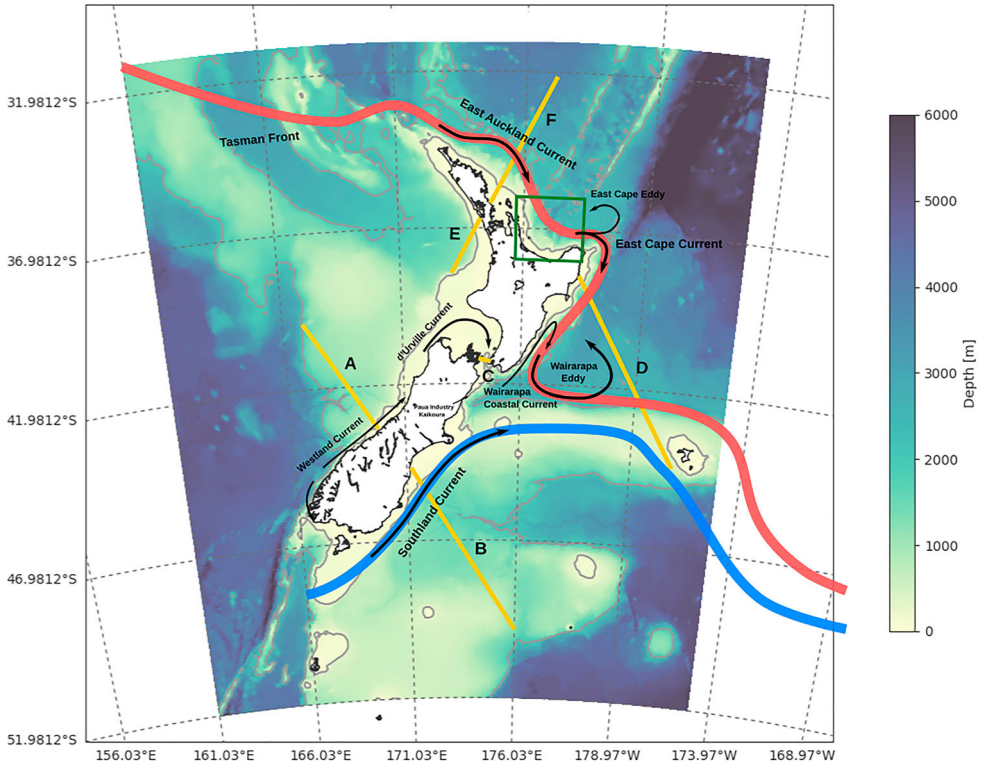

Figure 1. Map of the study area bathymetry, showing the main large scale currents that constitute the regional circulation. The transects where the circulation vertical structure and transport are analysed are presented in yellow. The green box shows the location of the Bay of Plenty, a region of particular economical significance used to exemplify the analysis of coastal processes. The red band links circulation from the Tasman Front, across the top of New Zealand North Island, and then along the top of Chatham Rise. While the blue band is the STF extension around the bottom of the South Island, and then along the south side of Chatham Rise.

boundaries to a national ocean model domain can then be evaluated. As stated in the work by Balmaseda et al. (2015), a sub-set of the publicly available reanalysis products were selected based on the inclusion of all the main variables usually needed as boundary conditions for nested ocean model domains, and their representation and focus on the New Zealand region. Therefore, the present work presents a comparison between the following four (near) global products: The 'Climate Forecast System Reanalysis' (CFSR), the 'Mercator Ocean Global Reanalysis' (GLORYS), the Reanalysis-2 based on the 'Hybrid Coordinate Ocean Model' (HYCOM) from the 'National Oceanic and Atmospheric Administration' (NOAA), and the Australian 'Bluelink Reanalysis' (BRAN).

The Ocean reanalyses

The reanalysis products considered herein use different ocean models with different assimilation schemes. In addition, they cover a different range of dates, resolution and geographic ranges and are regularly being updated. All of these factors act as uncertainty

sources when doing an inter-comparison. For example, Balmaseda et al. (2015) presents a compilation of the main products in use up until 2015. Notably missing from the assessment by Balmaseda et al. (2015) is BRAN, which was developed with a focus on Australia and New Zealand (Oke et al. 2013). Moreover, a new version of the Mercator reanalysis (GLORYS12v1) has been recently released, bringing important improvements over previous versions.

Therefore, the present study does not aim to be exhaustive, but to include the main products commonly used in both academia and industry in the southern hemisphere. A brief description of each of the reanalysis products assessed in this paper is presented below, and references are provided for the reader interested in further details.

Mercator reanalysis–GLORYS

In the present work we evaluate the results from the GLORYS version 12v1–the latest ocean reanalysis from the 'Copernicus Marine Environment Monitoring Service' (CMEMS) released in January 2019. It has 1/12° horizontal resolution and 50 vertical levels, representing a significant increase on the previous version's ability to resolve mesoscale variability (GLORYS4–1/4° horizontal resolution).

The reanalysis is generated using the 'Nucleus for European Modelling of the Ocean' (NEMO) ocean model driven at the surface by the ECMWF ERA-Interim reanalysis. It assimilates along track altimeter observations (sea level anomaly), satellite sea surface temperature (SST), sea ice concentration and *in situ* temperature and salinity vertical profiles from the '**C**oriolis **O**cean database **R**e**A**nalysis' (CORA) dataset (Szekely et al. 2019) using a reduced-order Kalman Filter scheme. In addition, it uses a 3D-Var scheme for the correction of large-scale biases in temperature and salinity. The reanalysis covers the satellite era from 1993 to 2018.

More details on GLORYS can be found in product page at the CMEMS website http://marine.copernicus.eu/services-portfolio/access-to-products/?option=com_csw&view=details&product_id=GLOBAL_REANALYSIS_PHY_001_030.

Bluelink reanalysis–BRAN

A full description of the BRAN ocean reanalysis is given by Oke et al. (2013). In the present work we analyse the results from BRAN2016 described by Zhang et al. (2016), due to the longer time series available (1993–2016). Comparisons with BRAN version 3p5 showed no significant differences over the overlaping time period.

BRAN is based on the GFDL Modular Ocean Model (MOM). The model presents a horizontal resolution of 1/10°, covering the region from 75°S to 75°N. It has 51 vertical layers, with 14 layers in the top 100 m, 19 layers between 100 m and 500 m, 6 layers from 500 m to 1000 m, and another 12 layers towards the bottom. BRAN does not include a sea-ice coupled model. The simulation is forced in the surface by 3-hourly fields from the Japanese 55-year reanalysis (Kobayashi et al. 2015) using bulk formula for wind stress, turbulent heat fluxes and evaporation. Observations are assimilated using an Ensemble Optimal Interpolation scheme named BODAS, described by Oke and Sakov (2008).

Access to the BRAN description and data is available at: https://wp.csiro.au/bluelink/global/bran/

NOAA reanalysis-2–HYCOM

The NOAA Reanalysis-2 is based on the HYCOM model using the Navy Coupled Ocean Data Assimilation (NCODA) as described by Cummings (2005). The HYCOM-NCODA product uses a multi-variate optimal interpolation scheme to assimilate satellite altimeter observations, satellite and *in situ* SST observations, as well as *in situ* vertical temperature and salinity profiles from XBTs, Argo floats and moored buoys.

The reanalysis has global coverage, with 1/12° horizontal resolution and 41 vertical layers. Over the history of the product there have been changes in model version, resolution, assimilated datasets, missing days, etc. Therefore, for consistency, only outputs from the experiments GLBu0.08 version 90.9 forward are used here, covering the period from May 2012 to November 2018.

The HYCOM reanalysis can be downloaded from https://www.hycom.org/dataserver.

Climate forecast system reanalysis–CFSR

The 'National Centers for Environmental Prediction' (NCEP) CFSR is a global coupled atmosphere/ocean/sea-ice reanalysis, with details provided by Saha et al. (2010). It covers the period from 1948 up to the present, the longest duration for all reanalyses available for the global ocean.

The CFSR ocean component is based on the Modular Ocean Model (MOM). It has a 1/2° zonal resolution and a variable meridional resolution: 1/4° between 10°S and 10°N, gradually decreasing to 1/2° poleward of 30°S and 30°N. The simulation has 40 vertical layers, being 27 in the upper 400 m of the water column. The reanalysis uses the GODAS 3DVar scheme (Derber and Rosati 1989) to assimilate temperature and salinity observations. The surface temperature is relaxed to the NOAA 1/4° optimal interpolation SST product (OISST–described below). Sea surface salinity is relaxed to the climatological value defined by the World Ocean Database 1998 described by Conkright et al. (1999).

Access to the data can be obtained at: https://climatedataguide.ucar.edu/climate-data/climate-forecast-system-reanalysis-cfsr

Observational datasets for model evaluation

To evaluate the reanalyses, a group of publicly available observational datasets was chosen, based on their spatial and temporal coverage and the representation of the regional dynamics. We describe them here.

Sea surface elevation–CMEMS products

To evaluate the general pattern of the mean circulation, the reanalyses were compared to the Mean Sea Surface (MSS) topography and Sea Level Anomaly (SLA) satellite composite products provided by CMEMS (Pujol and Mertz 2019). The MSS corresponds to a 20-year mean (1993–2012) based on altimetry data, provided at 1/60° resolution. The SLA is

provided as daily global maps on 1/4° resolution. We use the CMEMS 'all satellites' product which combines all the available along track observations at each time to provide the best possible estimate.

Sea surface temperature–NOAA OISST

To evaluate the performance in reproducing SST, which has key economic significance and public interest, we use the 'Advanced Very High Resolution Radiometer Sea Surface Temperature' (AVHRSST) optimal interpolation SST product (OISST) provided by NOAA (https://www.ncdc.noaa.gov/oisst). It consists of a 1/4° horizontal resolution daily product, that covers the period from late 1981 to the present. AVHRSST is limited by cloud coverage that can compromise the results, especially in coastal areas. Although a cloud-free product that includes infrared sensors is available, it covers a shorter time span from 2002 forward and is not used in the present work. More details on the product generation are provided by Reynolds et al. (2007).

Temperature and salinity profiles–CORA 5.2 dataset

The CORA 5.2 dataset described by Szekely et al. (2019) is used to evaluate the reanalyses representation of the water column structure. This dataset provides a global comprehensive collection of *in situ* temperature and salinity profiles from 1950 to 2017. It contains data from a diverse set of observational platforms, from mechanical bathythermographs (MBT) prior to 1965; expendable bathythermographs (XBT); conductivity, temperature and pressure sensors (CTD), etc. It includes all Argo float profiles from the late 1990s forward, which constitutes the majority of the data available for the New Zealand region. Therefore, most of the observations are limited to 2000 m deep–the maximum depth of regular Argo floats. There is a limited number of CTD casts that reach deeper layers in the study region, down to 4000 m. Although one can argue that the CORA dataset is assimilated by GLORYS, it consists mainly of Argo profiles assimilated by all reanalyses.

Results and discussion

Apart from the HYCOM reanalysis, all other products were compared for the period between January 1993 and the end of 2016. The selected HYCOM experiments start only in 2012, hence this start date was used. While this can have some effect on the analysis, it is expected to be minor. The comparisons were generated for the region between 52–31°S, and 161–185°E–corresponding to the oceanic region surrounding New Zealand (Figure 1).

Initially, the simulations were compared to satellite data to estimate the model skill in reproducing surface fields. It is expected that all simulations should compare well to satellite data as satellite observations dominate the data assimilated into each of the ocean models.

Comparisons against the CORA5.2 dataset are used to assess the reanalyses performance through the water column. Finally, 6 vertical sections were defined to analyse the

representation of the main boundary currents around New Zealand. The cross-section transports were calculated and are compared to previous studies.

Surface

All four reanalyses present the same MSS topography bias patterns (Figure 2). The models exhibit a sharper front for the Southland Current (SC), off the East coast of the South Island, and towards the East following the path of the Subtropical Front (STF). This is expected due to the simulations higher horizontal resolution compared to the MSS product. It is worth emphasising the representation of the STF is key to the regional dynamics and water mass structure. It corresponds to the eastward extension of the western boundary current, and the separation between the warmer and more saline Sub-tropical surface waters to the North from the cooler and fresher Sub-Antarctic waters to the South (Graham and De Boer 2013).

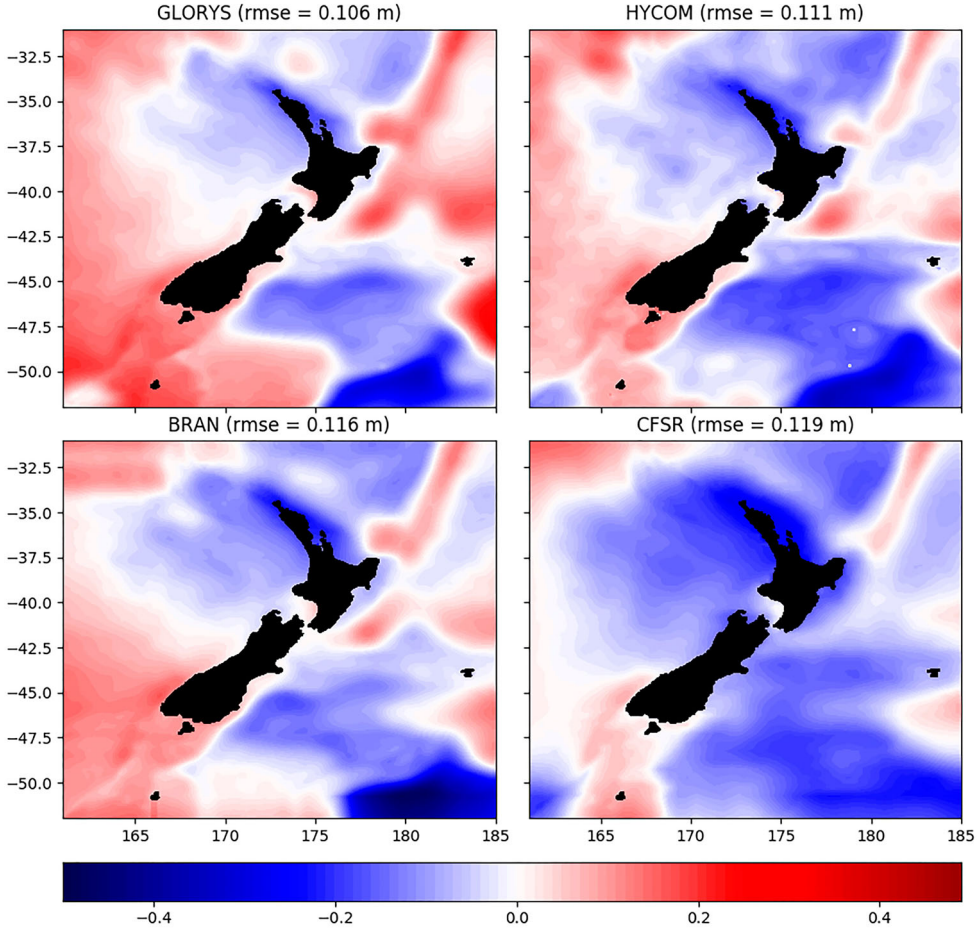

Figure 2. Difference between simulated and observed Mean Sea Surface topography (m) gridded product provided by Copernicus (model–observations). Model results were linearly interpolated to observations grid.

A similar behaviour is present for East Auckland Current (EAuC), off the East Coast of the North Island and around the East Cape (see map in Figure 1). Such differences, however, are smoother than the ones observed for the SC. This is a consequence of the presence of several eddy structures associated with the EAuC, while the SC has a more coherent flow. The root mean squared error (RMSE) is also similar between models, with GLORYS presenting a slightly smaller value. Based on these results, we conclude that all reanalyses products represent the mean large-scale circulation around New Zealand well.

Figure 3 presents differences between modelled and observed (AVISO) Sea Level Anomaly (SLA) variance. The errors are in the range of the global averages presented by Balmaseda et al. (2015). However, the zoom around New Zealand provides a better depiction of the spatial structure of the error in this region. While GLORYS reproduces the observed variance well, HYCOM tends to overestimate and BRAN underestimates it. Since a higher variance is expected for simulations with higher horizontal resolution,

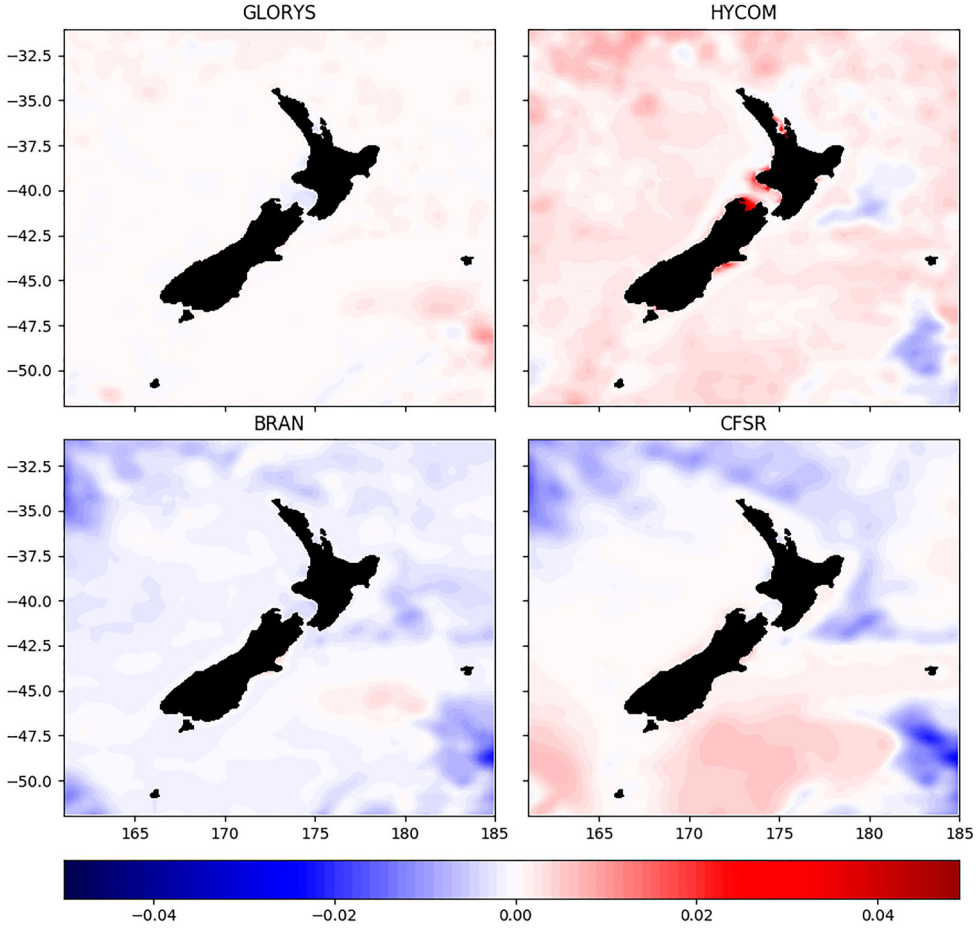

Figure 3. Difference between simulated and observed variance of the Sea Surface Height (m^2). Gridded product provided by Copernicus (model–observations). Model results were linearly interpolated to observations grid.

the underestimation by BRAN is surprising. The CFSR model overestimates the variability in SLA to the South of the STF and underestimates it to the North. This can have important consequences for mixing and water mass representation, specially for intermediate waters that are formed in this region.

While the analyses presented in Figures 2 and 3 provide a good overview of the robustness of the simulated Sea Surface Height (SSH), they do not provide any insight on how the variability behaves over time. Figure 4 shows the SLA first empirical orthogonal function (EOF) for the AVISO product and the reanalyses, expressed as the correlation with the total SLA variance. This first mode concentrates most of the variability, with the subsequent modes being relatively insignificant. All the models reproduce the general spatial pattern present in the AVISO product, as is expected from models that assimilate altimeter data. That is, a higher variability area connecting the SC, the EAuC and their extension through the STF. Both GLORYS and BRAN exhibit a good representation of smaller scale structures present in the observations. On the other hand the CFSR EOF spatial distribution is smoother than the observed, while HYCOM is noisier.

Looking at the temporal variability of the principal components (only 2 years are presented to emphasise the details), one can observe that GLORYS and BRAN show good agreement with the observations while CFSR tends to underestimate and HYCOM to overestimate the variability. This agrees well with the overestimated SLA variance exhibited by the HYCOM simulation in Figure 3. As shown by the spectra of the first mode principal component, there is variability concentrated on the annual period, and around the 180 and 90 days periods. Such pattern observed in the AVISO product is

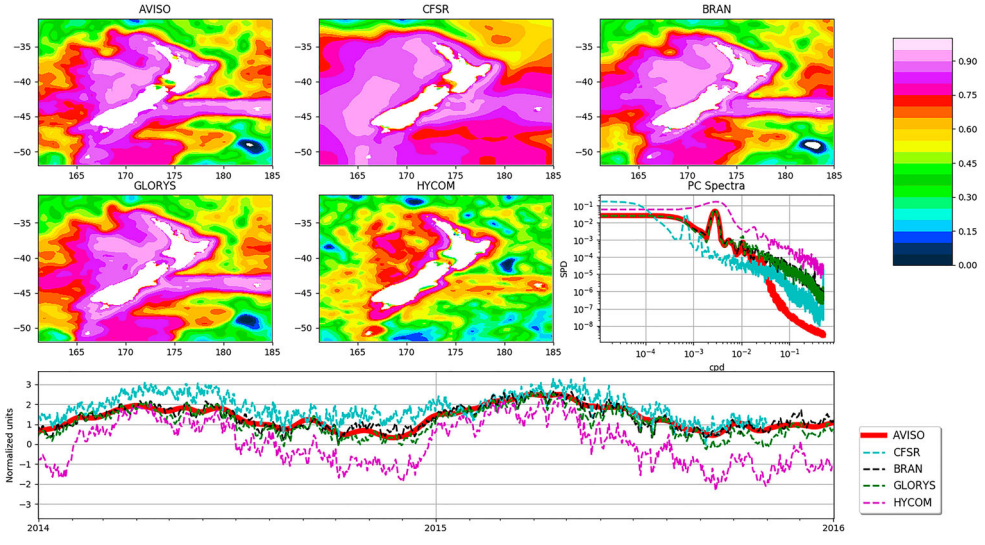

Figure 4. First empirical orthogonal functions of the Sea Level Anomaly expressed in terms of correlation. Top panels present the spatial patterns, and the spectra of the first mode principal component. While the temporal component (principal component) is presented in the lowest panel. Only the last 2 years of the time series is presented to emphasise the differences between simulations. The spectra of the first principal component (PC) shows that GLORYS and BRAN agree well with the observations. There is a clear peak corresponding to the seasonal cycle, and other two corresponding to periods of approximately 180 and 90 days. A hamming window with size 15 was used to smooth the spectra.

well reproduced in the GLORYS and BRAN reanalyses. While HYCOM does present a clear annual cycle with an overall higher energy for all frequencies, the spectra for the CFSR does not resemble the one for the observations with no clear spectral energy peaks. One should keep in mind that the AVISO product is the combination of different satellite passes through optimal interpolation, and tends to smooth out some scales. Due to the higher spatial resolution, the model simulations will present higher frequency and smaller scale eddies. It is interesting to notice how a large portion of the coastal ocean around New Zealand follows the seasonal cycle, with a particular strong variability in the west coast. This will have an impact on the ill defined coastal circulation in this area, as discussed bellow.

A major process driving the large scale variability around New Zealand corresponds to Rossby waves travelling westward and impinging onto New Zealand East coast, where they trigger Kelvin waves that propagate anti-clockwise around the islands. The mechanics of such wave-wave interaction have been described by Liu et al. (1999), and discussed within New Zealand context by Hill et al. (2010). The Hovmoller diagrams in Figure 5 clearly show this westward propagation of sea level perturbations in the AVISO product, reproduced by both GLORYS and BRAN reanalyses. Higher frequency variability is also noticeable, as expected of high resolution simulations. While the signal can be seen in the HYCOM results, it is not as clear due to the high level of noise. CFSR is unable to reproduce the observed planetary wave pattern.

The SST bias maps in Figure 6 present more insights into the regional dynamics. GLORYS overestimates the SST on most of the domain, with higher values for EAuC region and on the STF to the North of the Chatham Rise. A noticeable exception is the region of the SC and the STF to the South of the Chatham Rise. This may be due to the better defined current cores than depicted by the OISST, and agrees with the results

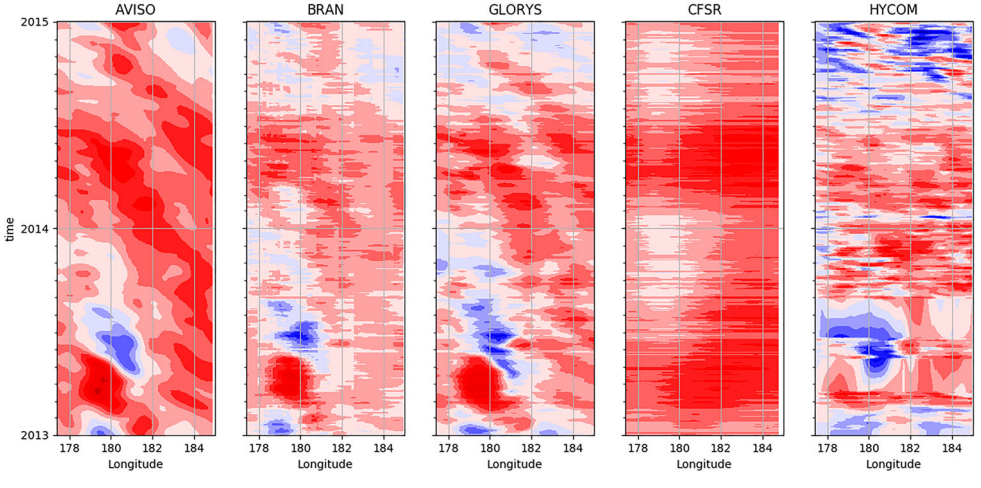

Figure 5. Space-time diagrams of the SLA along the 40°S parallel, for the AVISO gridded product and the four reanalyses. The contours are every 5 cm, from −40 cm (blue) to +40 cm (red). One can see a signal propagating westward in the observations and the BRAN and GLORYS simulations. The same signal is not evident in HYCOM and nonexistent in CFSR. The figure is zoomed in on the years 2013 and 2014 to emphasise the propagating perturbations.

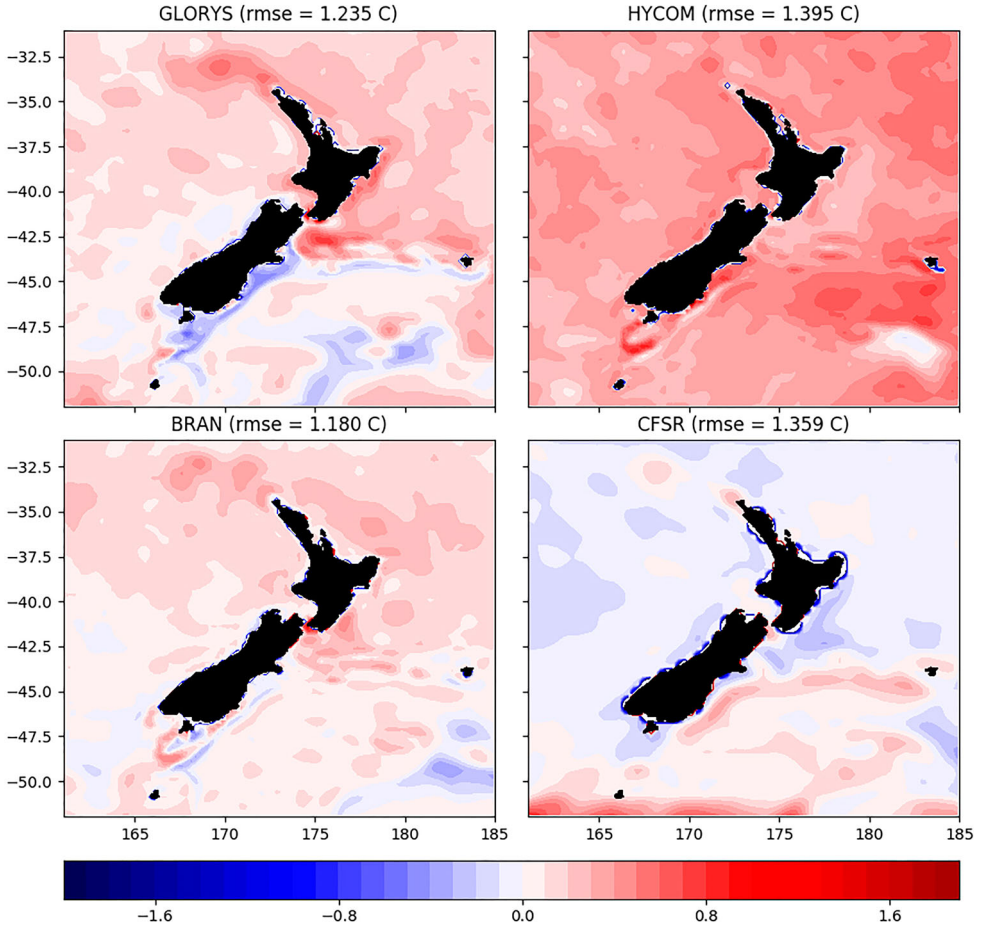

Figure 6. Difference between simulated and observed mean SST (°C) optimal interpolation product provided by NOAA (model–observations). Observations include only AVHRSST sensors. Model results were linearly interpolated to observations space.

for the SSH shown in Figure 2. However, this should be interpreted with caution, as the SST used is a lower resolution product of optimal interpolation of AHRSST observations that are highly sensitive to cloud coverage. BRAN exhibits a similar pattern to GLORYS, but with smaller overall SST RMSE.

Both HYCOM and CFSR have problems reproducing the regional SST. While HYCOM overestimates the SST in almost the whole domain, CFSR presents a similar trend in SST to the one observed in the SLA variance of Figure 3. This means CFSR is too warm to the south of the STF and too cold to the north, this can be related to limitations in resolving the cross-frontal heat flux at such resolution (0.5°). Interestingly, a similar spatial pattern was observed by Bull et al. (2018) for experiments where New Zealand and the Campbell Plateau were levelled to 4000 m deep. This demonstrates the importance of the New Zealand submarine platform in setting the spatial temperature structure, a process that can be misrepresented due to the low resolution in CFSR.

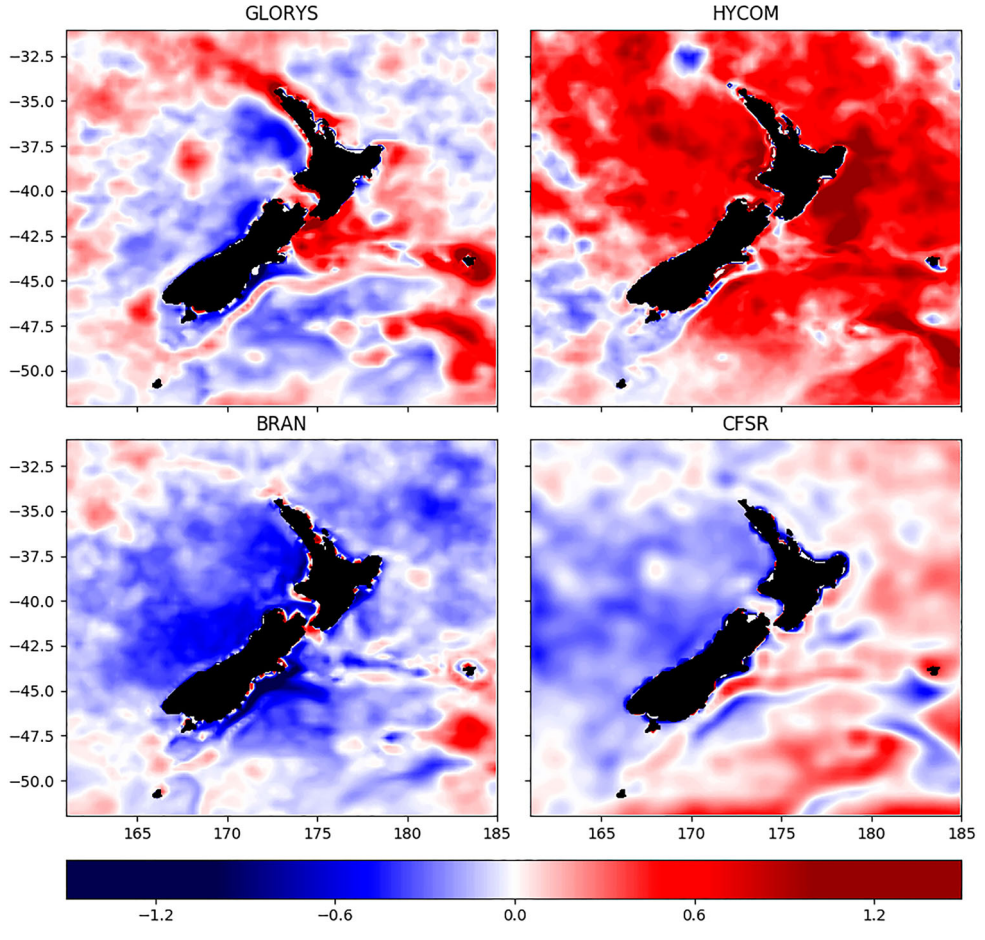

Figure 7. Difference between simulated and observed variance of the SST (°C) optimal interpolation product provided by NOAA (model–observations). Observations include only AVHRSST sensors. Model results were linearly interpolated to observations locations.

As expected, the SST variance differences in Figure 7 shows a similar pattern to the SLA variance differences in Figure 3. While HYCOM overestimates the variance across most of the domain, BRAN underestimates it. Particularly in the SC region, BRAN shows a large negative bias in the variance. GLORYS has higher variance in the area of the main large-scale currents, reflecting the simulation's higher resolution and stronger currents.

Water column

The vertical structure of the water column typically presents a challenge for ocean reanalysis products extending over a period of decades. Problems with spurious diffusion, biases introduced by forcing and lack of important physical processes have major consequences on the vertical distribution of temperature and salinity. Several of these are described by Kobayashi et al. (2015).

To evaluate the reanalyses performance in reproducing the water column structure, vertical profiles were co-located in time and space to coincide with all profiles available

in CORA 5.2 dataset. RMSE for both temperature and salinity were calculated considering all available profiles for each reanalysis (HYCOM covers a shorter time period), and are presented in Figure 8. It is clear that GLORYS performs better than the other simulations, showing smaller RMSE for both temperature and salinity through the water column. The only exception is the near-surface temperature RMSE that is slightly smaller in BRAN.

Interestingly, the temperature RMSE falls within the observed range for a regional reanalysis of the East Australian Current (EAC) presented by Kerry et al. (2016). Particularly since this region is dynamically connected to the EAC. There is a local maximum in the RMSE around 100 m, roughly corresponding to the base of the mixed layer. This suggests errors in the representation of the mixed layer depth by the simulations. Curiously, a similar vertical error distribution is observed by Balmaseda et al. (2015) in the inter-comparison of global ocean reanalyses in the Tropics. Bellow 100 m the errors generally decrease with depth reflecting the more stable and less stratified density structure. The exception is BRAN, which presents a larger error around 400 m that could be related to problems in representing the thermocline central waters.

The salinity presents generally higher RMSE values close to the surface than in depth, reflecting the difficulty that global models have in representing and including surface water fluxes and river inputs. The HYCOM salinity RMSE presents an interesting behaviour,

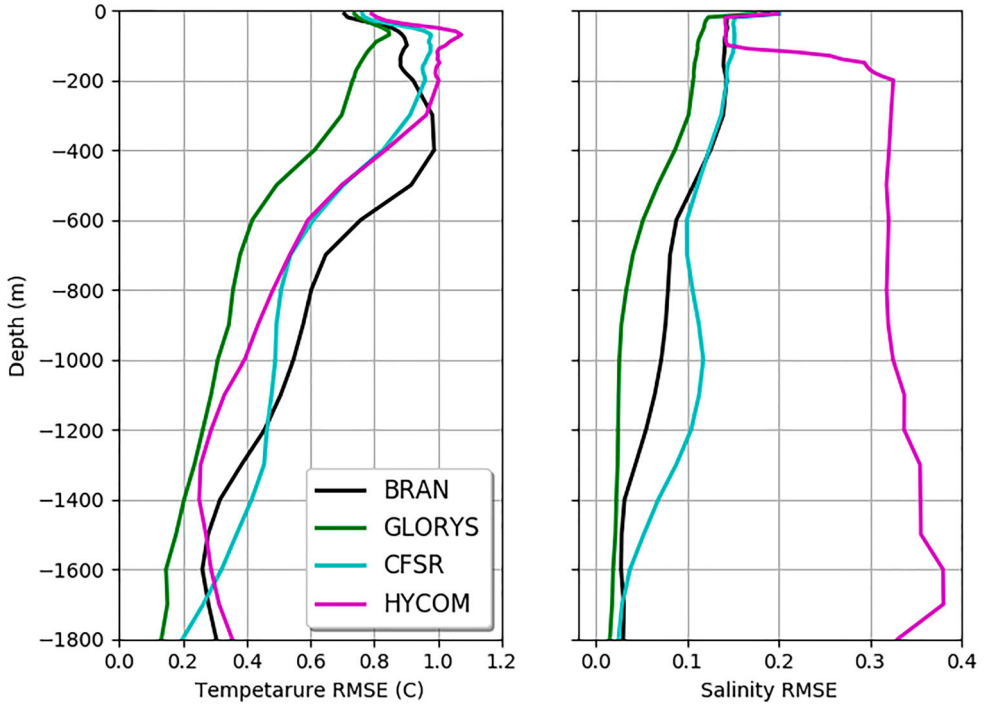

Figure 8. RMSE between the reanalyses solutions and the CORA observational dataset. The results are presented down to 1800 m to include only the depth range covered by the Argo floats. Argo data constitute the majority of the profiles available for this region in the CORA data set. It is interesting to note the large increase in salinity RMSE in the NOAA HYCOM reanalysis deeper than 100 m, although the cause is beyond the scope of this paper.

with a steep increase between 100 m and 200 m and an almost constant value below this depth.

Although useful, the RMSE temperature and salinity profiles in Figure 8 do not provide information on the spatial distribution of the error or the ability of the simulations to represent the regional and local dynamics. Therefore, the difference between modelled and observed temperature and salinity are presented in Figures 9 and 10 respectively. These maps were divided by depth layers corresponding approximately to the mixed layer (0–100 m), the thermocline (100–1000 m), the intermediate and deep waters (1000–2000 m), and a deeper layer including the few CTD profiles that reach under 2000 m (>2000 m).

The mean differences between modelled and observed temperature across the water column are $0.32 \pm 0.52^{\circ}$C for GLORYS and BRAN, $0.44 \pm 0.55^{\circ}$C for HYCOM, and $0.45 \pm 0.63^{\circ}$C for CFSR. Similarly, for the salinity the mean differences are 0.08 ± 0.14 for GLORYS, 0.10 ± 0.16 for BRAN, 0.11 ± 0.25 for HYCOM, and 0.12 ± 0.17 for CFSR. Individual profiles frequently present errors up to an order of magnitude larger than the mean values presented above.

All reanalyses behave similarly in the top layer(0-100m), particularly for temperature (Figure 9), with GLORYS and BRAN presenting overall smaller errors. The differences between modelled and observed temperature profiles in the surface layer are

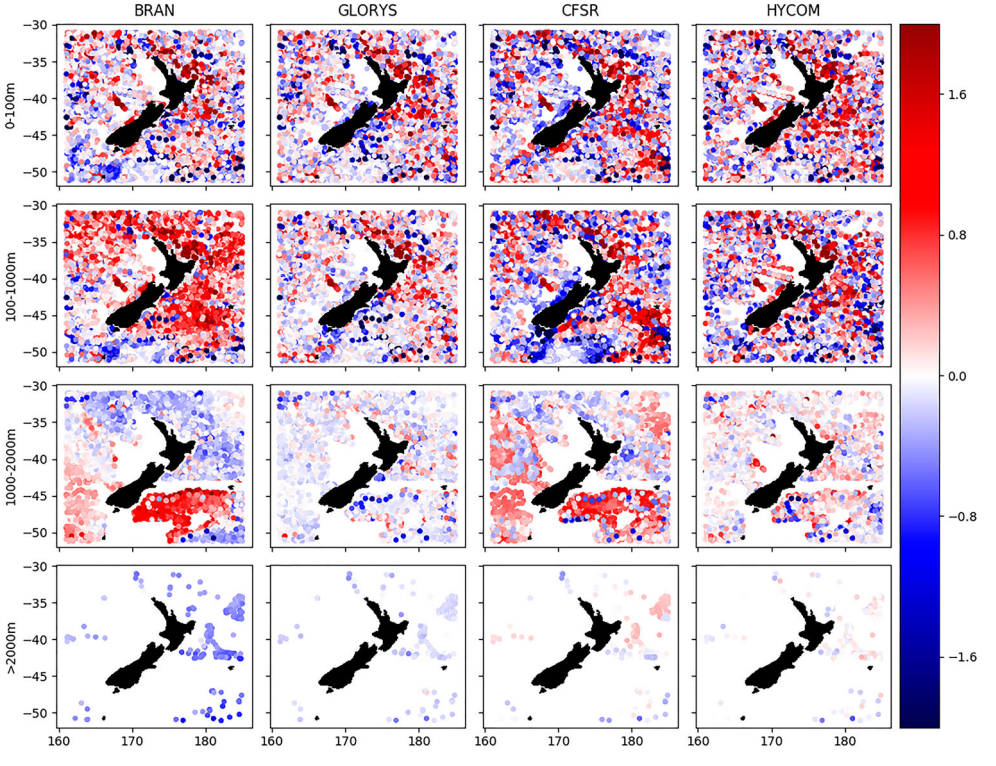

Figure 9. Difference between the temperature (°C) profiles in the CORA dataset and co-located reanalyses results (model–observations). Results are presented in depth slices, corresponding approximately to the mixed layer (0–100 m), the thermocline (100–1000 m), the intermediate and deep waters (1000–2000 m), and deep profiles (>2000 m).

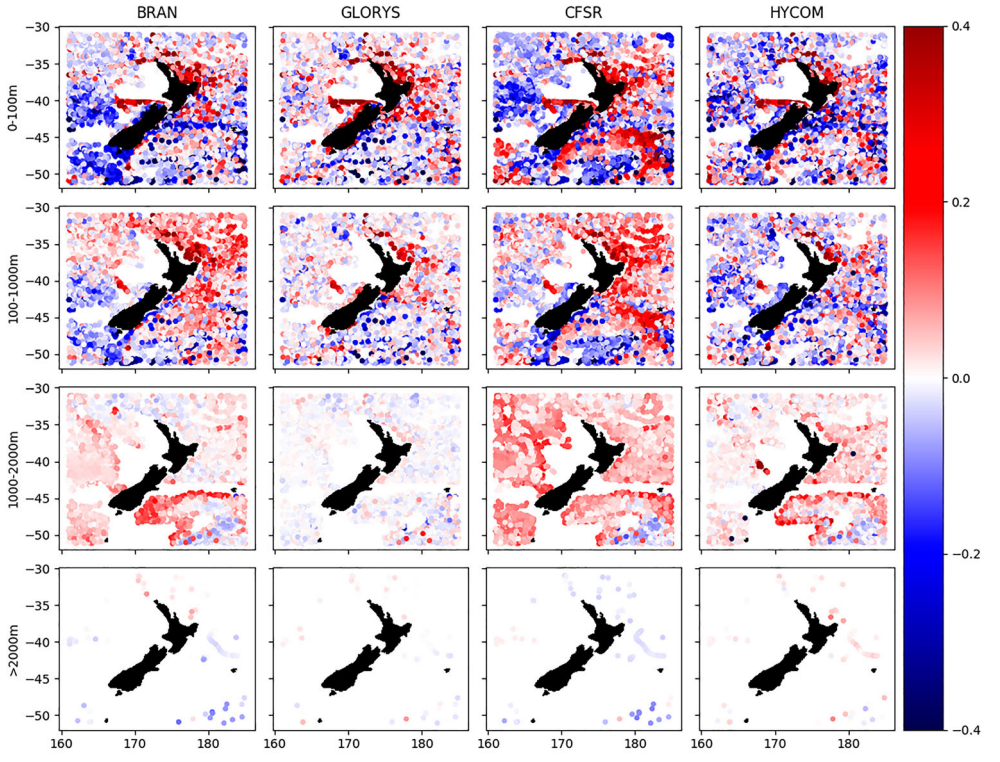

Figure 10. Difference between the salinity profiles in the CORA dataset and co-located reanalyses results (model–observations). Results are presented in depth slices, corresponding approximately to the mixed layer (0–100 m), the thermocline (100–1000 m), the intermediate and deep waters (1000–2000 m), and deep profiles (>2000 m).

0.45 ± 0.74°C for GLORYS and BRAN, 0.86 ± 0.56°C for HYCOM, and 0.55 ± 0.78°C for CFSR.

The performance of GLORYS stands out in the deeper layers, presenting overall smaller differences for both temperature and salinity than the other simulations. For example, in the 100–1000 m layer GLORYS presents differences of 0.37 ± 0.59°C and 0.06 ± 0.09, while the BRAN has shows biases of 0.53 ± 0.58°C and 0.09 ± 0.13, HYCOM 0.56 ± 0.59°C and 0.09 ± 0.28, and CFSR 0.58 ± 0.79°C and 0.10 ± 0.14 for temperature and salinity respectively. The errors are in general larger in the East of the domain, where the main currents are located and variability is larger.

The thermocline waters (100–1000 m) in the BRAN reanalysis are warmer than the observations (Figure 9), explaining the large mid-depth RMSE values. While in the 1000–2000 m layer, both BRAN and CFSR show waters warmer than observed to the south of the STF and cooler to the north. This can indicate problems in cross-frontal heat flux with potentially important consequences for representation of the meridional overturning circulation. There is a difference in the Antarctic Intermediate Water (AAIW) properties across the STF, being more saline and warmer in the model than in the observations to the north as observed by Chiswell et al. (2015) (see their Figure 2).

The comparison to the CORA dataset shows that both CFSR and BRAN are not able to reproduce this modification in the AAIW properties. The fact that the spatial domains of these reanalyses do not extend all the way to Antarctica (BRAN) or do it with relative low resolution (CFSR) may explain this limitation.

GLORYS shows lower salinity bias in the profiles in Figure 10. Particularly in the intermediate layers (100–1000 m and 1000–2000 m) where all the other reanalyses have positive salinity bias. Considering this in conjunction with the temperature difference maps (Figures 9), CFSR, BRAN and HYCOM present issues in reproducing the water mass structure in this region.

Velocity and transport sections

Previous efforts to evaluate the performance of global models in reproducing the regional circulation in the New Zealand region include (Chiswell and Rickard 2008) who evaluated an earlier version of 'Bluelink Reanalysis' (BRAN–version 2.1). They compared Eulerian and Lagrangian statistics and energy spectra in the model against observations and showed that the model compares fairly well to surface observations in the NZ region. In an attempt to validate BRAN at depth, Chiswell and Rickard (2014) compared model output with surface and 1000 m velocities from drifters and argo floats. They show that at depth BRAN is generally too strong at low latitudes and too weak at high latitudes.

In the present work, a different approach was chosen to access performance in reproducing the ocean currents. Six velocity transects (Figure 1) were extracted from each of the reanalyses to examine their representation of the regional circulation. The transects correspond to (A) the Westland Current (WC), (B) the Southland Current (SC), (C) the Cook Strait, (D) the East Cape Current (ECC), (E) the circulation on the west coast of the North Island, and (F) the EAuC. The transect positions where chosen to match the altimeter tracks used by Fernandez et al. (2018) to evaluate the mean transport of the ocean boundary currents (hence are not shore normal). Transport time series were calculated for all transects.

The mean and standard deviation (std) of cross-section velocities are presented in Figures 11 and 12, respectively. The differences between reanalyses is striking, in particular for the Cook Strait (Section C). In BRAN it corresponds to only 2 grid cells. The main regional currents (Figure 11) present in general larger magnitudes and sharper fronts in GLORYS: WC in Section A, SC in section B, and the EAuC in sections D and F. HYCOM presents similar mean currents to GLORYS, in particular in sections D and F (the ECC and EAuC). There are important differences in the way each model represents the bathymetry, with CFSR not being able to place the shelf break due to the lack of resolution. As a consequence, CFSR present boundary currents that are weaker, broader, and ill placed when compared to the other 3 simulations.

In general, HYCOM presents higher variability compared to the remaining simulations (Figure 12). This means that the high variability observed in Figures 3 and 7 actually covers the whole water column. GLORYS presents an overall higher variability when compared to BRAN, but lower than HYCOM. Once more, CFSR results show this simulation is not capable of representing the variability associated with the boundary currents around New Zealand.

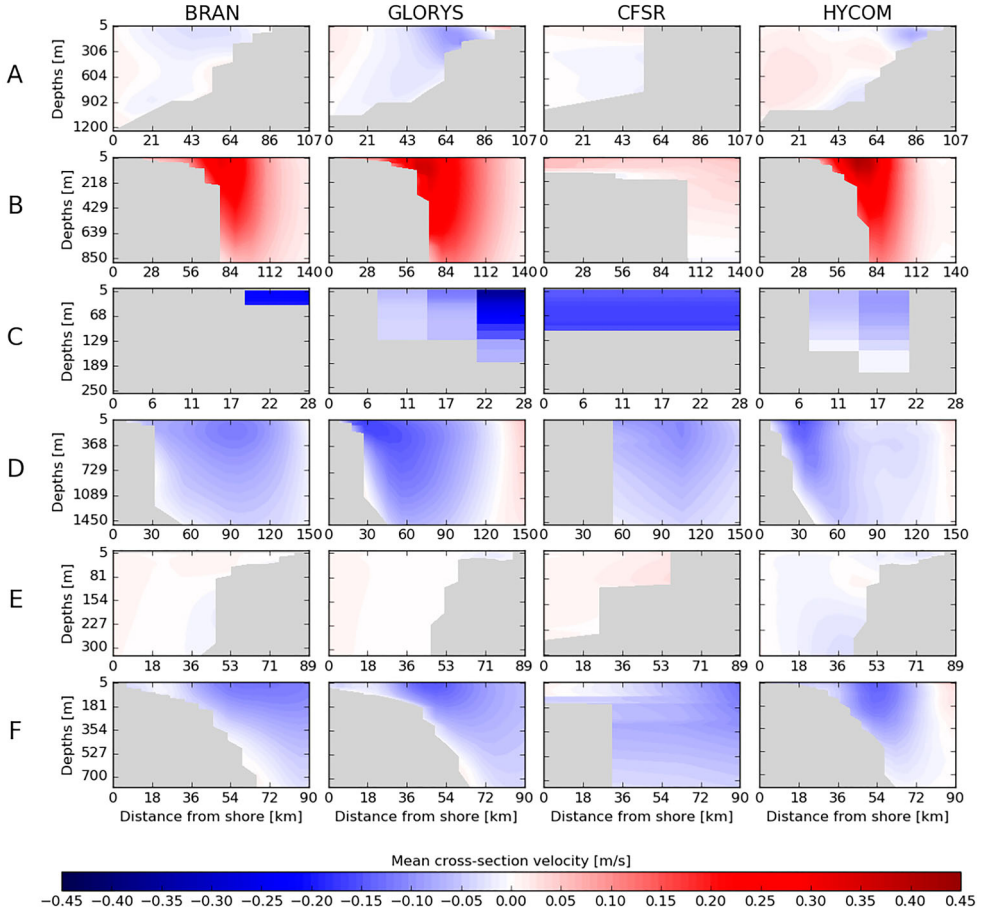

Figure 11. Mean velocities [m/s] across sections A (WC), B (SC), C (Cook Strait), D (ECC), E (west coast of the North Island) and F (EAuC) derived from BRAN (22-year), GLORYS (24-year), CFSR (39-year) and HYCOM (6-year) datasets. Negative values represent southward flow while positive values represent northward flow.

Transport time series were calculated for each vertical section as displayed in Figure 11. Because of differences in horizontal resolution, grid cell locations and bathymetric representation among the reanalysis products, both horizontal and vertical extents of each section had to be defined through visual identification of the mean current core location followed by a manual adjustment in order to minimise the cross-sectional area differences between products. Hence, transport estimates should be interpreted with care, but it is believed to be a reasonable compromise and still provide some insight on how each product resolve the regional boundary currents. Transport time series for CFSR are not presented since this simulation does not have the appropriate horizontal resolution to resolve those features at the given spatial scales.

Transport time series for the 3 reanalyses are illustrated in Figure 13, along with its respective mean and std values (Table 1). Positive values indicate northward transport as for section B where SC is represented, while negative values indicate southward transports such as EAuC and ECC represented in sections F and D, respectively.

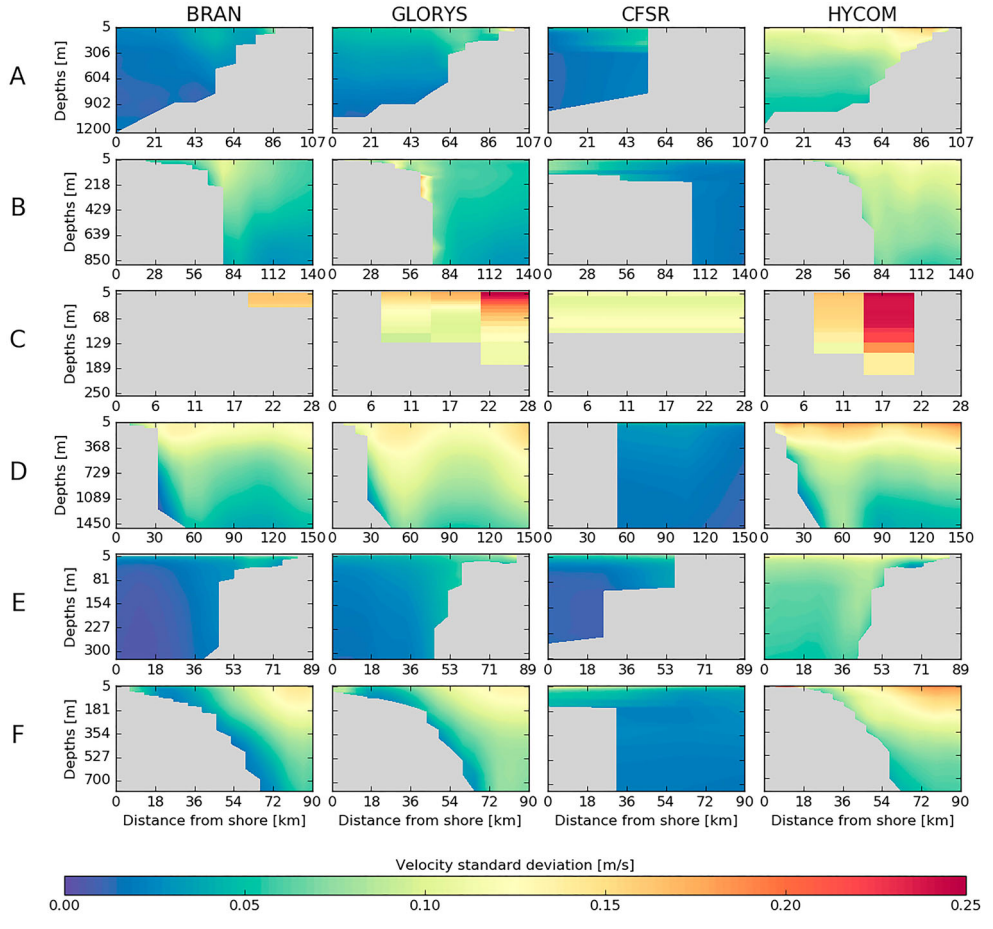

Figure 12. Standard deviation calculated from daily averaged velocities across sections A (WC), B (SC), C (Cook Strait), D (ECC), E (west coast of the North Island) and F (EAuC) derived from BRAN (22-year), GLORYS (24-year), CFSR (39-year) and HYCOM (6-year) datasets.

Mean transport estimates at section B, corresponding to the SC current, shows GLORYS, BRAN and HYCOM in the same order of transport values presented in Fernandez et al. (2018) (10.6 $\pm$ 1 Sv), while GLORYS and HYCOM estimates are closer to those obtained from CTD measurements to the south of the section position (8.5 $\pm$ 2.3 Sv). At section F (EAuC), transport values from BRAN are in agreement with the estimates presented in Fernandez et al. (2018) (10.5 $\pm$ 2.7 Sv). Both GLORYS and HYCOM underestimate transport at the location. These differences in the transport may in part be explained by the focus put into BRAN in resolving the EAC, ultimately forming the Tasman Front and the EAuC. On the other hand, estimates from section F (ECC) reveals GLORYS and HYCOM being much closer to the results presented in Fernandez et al. (2018) (10.5 $\pm$ 2.7 Sv) while BRAN shows transport values 3 times higher (32.50 $\pm$ 16.67 SV) than satellite estimates. These values suggest such discrepancies are enhanced by the transport calculation being carried over a much bigger area than the actual boundary current core, given the larger extents of this particular section compared

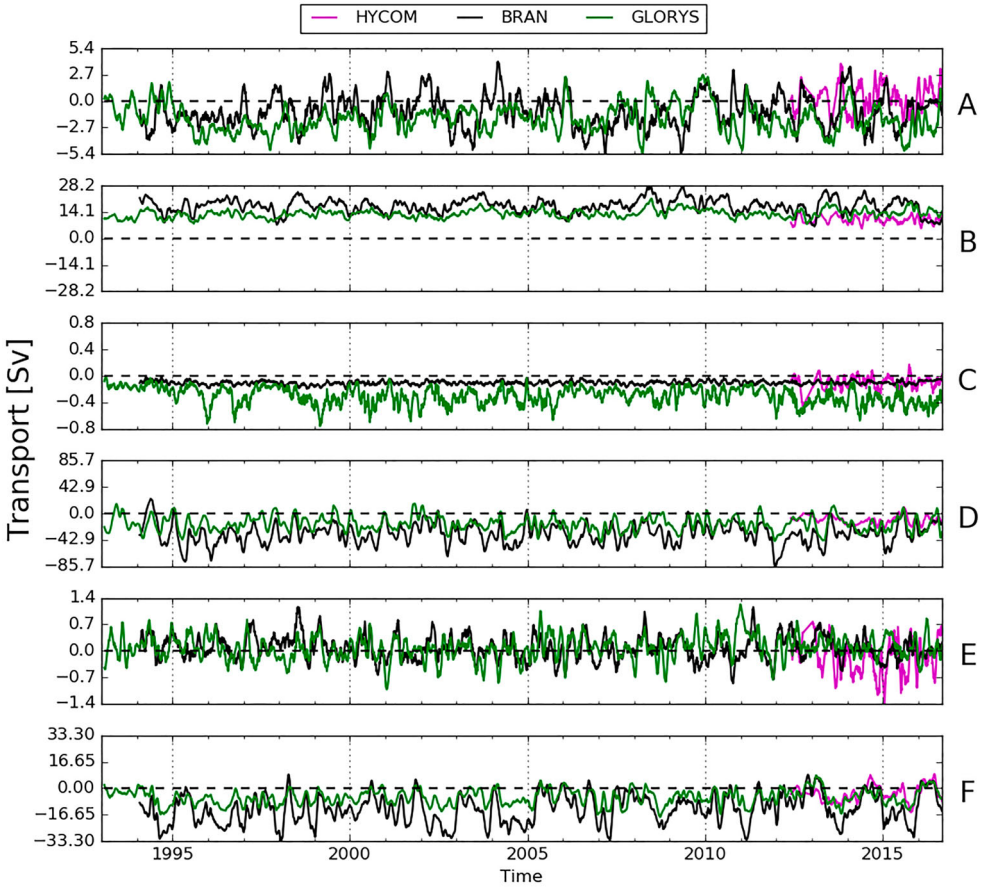

Figure 13. Time series of daily averaged transport [Sv] across sections A (WC), B (SC), C (Cook Strait), D (ECC), E (west coast of the North Island) and F (EAuC). Negative values represent southward transport while positive values represent northward transport. Coloured lines are transport estimated from HYCOM (magenta), BRAN (black) and GLORYS (green) datasets. Time series are truncated from 1993 to 2018 and low-pass filtered using 31-days window for better visualisation.

Table 1. Mean cross-section transport (Sv) from the 3 reanalysis products.

	GLORYS		BRAN		HYCOM	
	Mean	Std	Mean	Std	Mean	Std
A	−1.77	1.44	−1.06	1.66	0.39	1.37
B	13.20	2.19	17.46	3.86	10.08	1.98
C	−0.30	0.12	−0.10	0.02	−0.11	0.10
D	−16.88	12.0	−32.50	16.67	−10.25	6.73
E	0.08	0.32	0.07	0.31	−0.14	0.47
F	−5.73	4.76	−13.02	9.17	−3.15	4.89

to the remaining ones. Note that the differences between the three reanalysis are consistent with transport seen at the EAuC representative section.

It is interesting to observe how the simulated transport variability for all simulations agree well in the West coast of New Zealand (sections A and E). This area presents a

particularly strong variability with a pronounced seasonal cycle, as evident in the SLA EOF in Figure 4. All reanalyses show a mean transport in the opposite direction as one would expect for the WC (section A), indicating the inability in represent this coastal current. While in section E the models show a variable current with no defined direction. While the Cook Strait is not well resolved in any of the reanalyses, GLORYS transport values are closer to the estimates presented in Stevens (2014). Both BRAN and HYCOM underestimate the mean transport across the strait, with BRAN exhibiting less pronounced variability as seen in the other 2 simulations.

Representation of coastal processes

Global products are not expected to produce coastal processes well. Hence the need for regional downscaling if one is interested in coastal regions. To illustrate this point, particularly poor performance can be observed for all 4 reanalyses for key coastal processes. For example, the Three Kings Islands upwelling along the northern tip of the North Island (Stanton 1973) is not properly represented in any simulation. This is evident by the large positive error (warm waters) present in all reanalyses in this region (Figure 6). The absence of this process can be related to its small scale, under the resolution of the simulations, and the bathymetry representation. However, it influences the temperature structure over a larger area as shown by the OISST product. In addition, Figures 9 and 10 show large errors in the temperature and salinity vertical structure along the EAuC path.

To illustrate the inability of the global simulations in representing coastal areas, Figure 14 presents a zoom in the differences between the temperature and salinity profiles for GLORYS–the simulation with the most accurate vertical structure–in the Bay of Plenty region (green box in Figure 1). Considering the whole water column, the differences are $0.24 \pm 0.77^{\circ}$C for the temperature, and 0.07 ± 0.14 for the salinity. Large error values

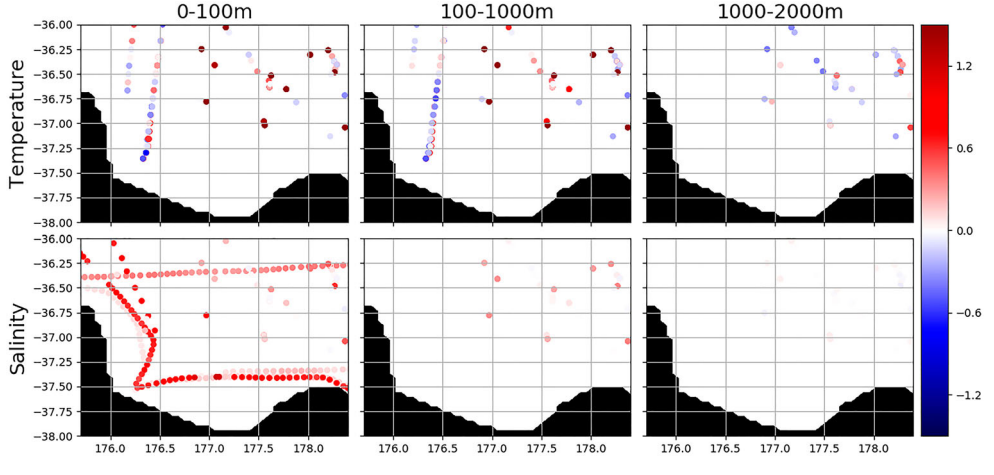

Figure 14. Difference between the temperature (°C) and salinity profiles in the CORA dataset and co-located GLORYS results for the Bay of Plenty region (model–observations). Results are presented in depth slices, corresponding approximately to the mixed layer (0–100 m), the thermocline (100–1000 m), and the intermediate and deep waters (1000–2000 m).

(4.17°C and 0.75) can be observed in the mixed layer and thermocline. These may be related to the relative low resolution to properly resolve coastal processes, and the lack of important physical processes such as freshwater input by local rivers and tidal mixing. This result emphasises the caution needed when using global reanalysis products for coastal applications.

Conclusions

We present an assessment of 4 publicly available (near) global ocean reanalyses with the purpose of understanding the optimal product for providing open boundary conditions for regional models for New Zealand waters. Our results show that while all models perform reasonably well in the surface waters (where data assimilation has maximum benefit), there are important differences in the ocean interior. While GLORYS shows good agreement with the vertical profile observations, the same is not true for the remaining reanalyses. These models have difficulty in representing the thermocline structure. Moreover, both BRAN and CFSR show limitations in resolving the meridional overturning circulation, leading to intermediate and deep waters that are too warm to the south and too cold to the north of the Subtropical Front.

One should keep in mind that the fact that GLORYS assimilates CORA influences the analysis results. However, the largest dataset of vertical profiles–the Argo floats–is assimilated in all the reanalyses. Therefore, any bias in the evaluation is expected to be minor. The large misfit with the profiles presented by CFSR, HYCOM, and BRAN in the deep waters that can not be attributed to any analysis bias. Ideally, independent observations should be used to evaluate the simulations. This is based on the assumption that the assimilation process will improve the representation of the regional dynamics, affecting the wider domain and other non-assimilated variables. However, such simulations are designed to assimilate all available observations. The remaining non-assimilated datasets are generally scarce in time and limited to the coast, being of little value for a regional comparison.

The reanalyses are able to capture the main boundary currents around New Zealand: from north to south, the East Auckland Current (EAuC), the East Cape Current (ECC), and the Southland Current (SC). GLORYS show overall stronger and more variable currents, with sharper fronts on their edges. However, CFSR exhibits limitations related to the horizontal resolution to represent the main boundary currents. Therefore, the transport results for this reanalysis are not discussed.

Compared to Fernandez et al. (2018), the transport of the EAuC is underestimated in both GLORYS and HYCOM. While BRAN overestimates it, the values are closer to published estimates. Again for the SC, BRAN underestimate the transport while GLORYS and HYCOM are much closer, although values are slightly higher. For this current, however, all simulations present results that approximate the estimates from satellite altimeter data from Fernandez et al. (2018). All simulations have problems in representing the weaker coastal fluxes in the west coast of New Zealand, and the flux through the Cook Strait. GLORYS does a better job compared to the other simulations, but is still not able to reproduce the coastal flow. This comparison results must be interpreted with care since Fernandez et al. (2018) uses a more sophisticate method to identify the current borders to calculate the transport, while we use fixed sections.

Overall the GLORYS reanalysis performs best for most of the analyses presented here, and is therefore recommended as source of boundary conditions for regional model simulations. However, its use to provide a best guess circulation for direct use in coastal applications around New Zealand is not advised. None of the reanalyses show a good representation of the coastal circulation, and even GLORYS presents large errors when contrasted to the temperature and salinity profiles in the Bay of Plenty. The lack of representation of coastal sources of fresh water seems to be a deficiency of all global reanalyses, with important consequences on the representation of shelf water column structure and dynamics.

Our results show that, to support industry and societal applications, there is a clear need for the development of regional downscaled models around New Zealand based on global ocean reanalysis products. These downscaled models should include physical processes that are not represented in the global simulations, such as tidal and local wind and atmospheric pressure forcing, and better resolve the continental shelf bathymetry and coastal geometry.

Acknowledgments

The Ssalto/Duacs altimeter products and the CORA dataset were produced and distributed by the Copernicus Marine and Environment Monitoring Service (CMEMS) (http://www.marine.copernicus.eu).

Disclosure statement

No potential conflict of interest was reported by the authors.

Funding

This work is a contribution to the Moana Project (www.moanaproject.org), funded by the New Zealand Ministry for Business Innovation and Employment, contract number METO1801.

ORCID

Joao Marcos Azevedo Correia de Souza http://orcid.org/0000-0001-7745-157X

References

Balmaseda MA, Hernandez F, Storto A, Palmer MD, Alves O, Shi L, Smith GC, Toyoda T, Valdivieso M, Barnier B, et al. 2015. The ocean reanalyses intercomparison project (ORA–IP). Journal of Operational Oceanography. 8(supp1):s80–s97.

Bull YS, Kiss AE, van Sebille E, Jourdain NC, England MH. 2018. The role of the New Zealand plateau in the tasman sea circulation and separation of the east australian current christopher. Journal of Geophysical Research: Oceans. 123(2):1457–1470.

Callaghan JO, Stevens C, Roughan M, Cornelisen C, Sutton P, Garrett S, Giorli G, Smith RO, Currie KI, Suanda SH, et al. 2019 Mar. Developing an integrated ocean observing system for New Zealand. Frontiers in Marine Science. 6:1–7.

Chiswell SM, Bostock HC, Sutton PJH, Williams MJM. 2015. Physical oceanography of the deep seas around New Zealand: a review. New Zealand Journal of Marine and Freshwater Research. 49:286–317.

Chiswell SM, Rickard GJ. 2008. Eulerian and lagrangian statistics in the bluelink numerical model and aviso altimetry: validation of model eddy kinetics. Journal of Geophysical Research–Oceans. 113:1–14.
Chiswell SM, Rickard GJ. 2014. Evaluation of bluelink hindcast bran 3.5 at surface and 1000 m. Ocean Modelling. 83:286–317.
Conkright ME, Levitus S, O'Brien T, Boyer TP, Stephens C, Johnson D, Baranova O, Antonov J, Gelfeld R, Rochester J, et al. 1999. World ocean database 1998, documentation and quality control version 2.0. National Oceanographic Data Center. Report No.
Cummings JA. 2005. Operational multivariate ocean data assimilation. Quarterly Journal of the Royal Meteorological Society. 131(613):3583–3604.
Derber J, Rosati A. 1989. A global oceanic data assimilation system. Journal of Physical Oceanography. 19:1333–1347.
Fernandez D, Bowen M, Sutton P. 2018. Variability, coherence and forcing mechanisms in the New Zealand ocean boundary currents. Progress in Oceanography. 165:168–188.
Graham RM, De Boer AM. 2013. The dynamical subtropical front. Journal of Geophysical Research: Oceans. 118:5676–5685.
Hill K, Rintoul S, Oke PR, Ridgway K. 2010. Rapid response of the east australian current to remote wind forcing: the role of barotropic-baroclinic interactions. Journal of Marine Research. 68:413–431.
Kerry C, Powell B, Roughan M, Oke P. 2016. Development and evaluation of a high-resolution reanalysis of the east australian current region using the regional ocean modelling system (ROMS 3.4) and incremental strong-constraint 4-dimensional variational (IS4D-VAR) data assimilation. Geoscientific Model Development. 9:3779–3801.
Kobayashi S, Ota Y, Harada Y, Ebita A, Moriya M, Onoda H, Onogi K, Kamahori C, Endo H, Miyaoka K, et al. 2015. The JRA-55 reanalysis: general specifications and basic characteristics. Journal of the Meteorological Society of Japan. 93:5–48.
Liu Z, Wu L, Bayler E. 1999. Rossby wave–coastal Kelvin wave interaction in the extratropics. Part I: Low-frequency adjustment in a closed basin. Journal of Physical Oceanography. 29:2382–2404.
Moore AM, Martin MJ, Akella S, Arango HG, Balmaseda M, Bertino L, Ciavatta S, Cornuelle B, Cummings J, Frolov S, et al. 2019. Synthesis of ocean observations using data assimilation for operational, real-time and reanalysis systems: a more complete picture of the state of the ocean. Frontiers in Mrine Science. 6:90.
Oke PR, Sakov P. 2008. Representation error of oceanic observations for data assimilation. Journal of Atmospheric and Oceanic Technology. 25:1004–1017.
Oke PR, Sakov P, Cahill ML, Dunn JR, Fiedler R, Griffin DA, Mansbridge JV, Ridgway KR, Schiller A. 2013. Towards a dynamically balanced eddy-resolving ocean reanalysis: BRAN3. Ocean Modelling. 67:52–70.
Pujol MI, Mertz F. 2019. Product user manual for sea level sla products. EU Copernicus Marine Service. Report No. Available from: http://resources.marine.copernicus.eu/documents/PUM/CMEMS-SL-PUM-008-032-062.pdf.
Reynolds RW, Smith TM, Liu C, Chelton DB, Casey KS, Schalax MG. 2007. Daily high-resolution-blended analyses for sea surface temperature. Journal of Climate. 20:5473–5496.
Saha S, Moorthi S, Pan H, Wu X, Wang J, Nadiga S, Tripp P, Kistler R, Woollen J, Behringer D, et al. 2010. The ncep climate forecast system reanalysis. Bulletin of the American Meteorological Society. 91(8):1015–1057.
Stanton BR. 1973. Hydrological investigations around Northern New Zealand. New Zealand Journal of Marine and Freshwater Research. 7:85–110.
Stevens C. 2014. Residual flows in cook strait, a large tidally dominated strait. Journal of Physical Oceanography. 44:1654–1670.
Stevens C, O'Callaghan JM, Chiswell SM, Hadfield MG. 2019. Physical oceanography of New Zealand/Aotearoa shelf seas–a review. New Zealand Journal of Marine and Freshwater Research. 53:201–221.

Szekely T, Gourrion J, Pouliquen S, Reverdin G. 2019. The CORA 5.2 dataset: global in-situ temperature and salinity measurements dataset. Data description and validation. Ocean Science Discussion.

Zhang X, Oke PR, Feng M, CHamberlain MA, Church JA, Monselesan D, Sun C, Matear RJ, Schiller A, Fiedler R. 2016. A near-global eddy-resolving OGCM for climate studies. Geophysical Model Development Discussions.